



## Perspectives

## The role of isolated nitrogen in phosphorescence of high-temperature-high-pressure synthetic type IIb diamonds

Tian Shao<sup>a,1</sup>, Fanglin Lyu<sup>a,1</sup>, Xuewen Guo<sup>b</sup>, Jinqiu Zhang<sup>a</sup>, Haikun Zhang<sup>a</sup>, Xin Hu<sup>b</sup>, Andy H. Shen<sup>a,\*</sup><sup>a</sup> School of Materials Science and Engineering, Beijing University of Aeronautics and Astronautics, Beijing 100191, China<sup>b</sup> School of Materials Science and Engineering, Beijing University of Aeronautics and Astronautics, Beijing 100191, China

## ARTICLE INFO

Received 9 December 2019  
 Received in revised form  
 4 May 2020  
 Accepted 22 May 2020  
 Available online 27 May 2020

## ABSTRACT

Donor-acceptor pair recombination theory was used extensively to explain type IIb diamond phosphorescence mechanism, in which the acceptor was widely believed to be boron, and the donor remained an issue of debate. In this work, 10 pieces of high-temperature-high-pressure synthetic diamonds were studied by using DiamondView™, Fourier transform infrared spectroscopy, photoluminescence spectroscopy and electron paramagnetic resonance (EPR) spectroscopy. All the samples presented greenish blue phosphorescence, with emission band centered at 470 nm with a ~500 nm shoulder, which can be excited by ultraviolet light with wavelengths from 215 to 240 nm. A neutral isolated nitrogen signal appeared in EPR when the sample was illuminated with a short wave ultraviolet light source. These results helped us to suggest the isolated nitrogen is the most likely donor to generate phosphorescence with boron.

© 2020 Elsevier Ltd. All rights reserved.

## 1. Introduction

Diamond is a material composing only covalently bonded carbon (C) atoms. With high hardness, high refractive index, high thermal conductivity and other extraordinary physical and chemical properties, diamond has always been a significant material in several science and technology fields. Pure diamond is colorless, but impurities trapped in diamond may change its color and other physical properties. Typical impurities are nitrogen (N) and boron (B). Some nitrogen-related defects absorb light in ultraviolet region, then extend to the blue-purple region and make diamonds appear yellowish in color [1]. Boron-related centers can produce blue color in diamond by absorbing light ranged from near-infrared to red region [2,3]. Diamond doped with boron is a p-type semiconductor and classified as type IIb diamond [4–7]. This kind of natural semiconductor diamonds were discovered in the 1950s [6]. Hall effect and neutron activation experiments confirmed that boron is the only reasonable impurity responsible for the conductivity [8–10]. Using Fourier transform infrared (FTIR) spectroscopy, type

IIb diamond can be identified, and further, concentration of uncompensated boron can be determined [11].

High-temperature-high-pressure (HPHT) method was utilized to synthesize various types of diamonds successfully [12]. Existence of nitrogen in atmosphere made nitrogen-related impurities nearly unavoidable in HPHT synthetic diamonds. To obtain diamonds with less yellow color, nitrogen getter such as alumina (Al) and zirconium (Zr), or boron were added during the synthetic process to restrain the nitrogen concentration [12,13]. Those boron-doped HPHT synthetic diamonds are blue or colorless, and still can be classified as type IIb using FTIR spectra.

Boron doping also allows diamonds to produce phosphorescence centered in 500 nm when excited by shortwave ultraviolet light (UV-light). In previously published literatures, many [14–17] believed this phosphorescence could be explained by donor-acceptor pair recombination (DAPR) theory, which can be expressed by the following equation:

$$E(r) = \frac{1}{4} \left( \frac{E_{\text{ph}} - E_{\text{a}} - E_{\text{d}}}{e} \right)^2, \quad \text{Eq.1}$$

where  $E_{\text{ph}}$  is phosphorescent photon energy,  $E_{\text{a}}$  is the width of diamond bandgap,  $E_{\text{a}}$  is the binding energy of acceptor (above the valence band maximum),  $E_{\text{d}}$  is the binding energy of donor

\* Corresponding author.

E-mail address: [shenxt@cug.edu.cn](mailto:shenxt@cug.edu.cn) (A.H. Shen).<sup>1</sup> T. Shao and F. Lyu contribute equally.

(below the conduction band minimum),  $e$  is the electron charge,  $\epsilon$  is the electrostatic dielectric constant of diamond, and  $r$  is the distance between donor and acceptor.

At the beginning, DAPR theory was suggested to explain the luminescence phenomenon caused by acceptor-to-donor excitation in zinc sulfide (ZnS) and gallium phosphide (GaP) [18–20]. Since the phosphorescence of type IIb diamond has similar band shape and other optical properties to those in ZnS and GaP, DAPR theory was then applied to interpret phosphorescence phenomenon in type IIb diamonds in 1965 [14]. In this theory, donor and acceptor both participate to generate the luminescence. To this day, boron is believed to be the acceptor [10,21] and its binding energy was measured to be 0.37 eV above the valence band maximum (VBM). But the nature of donor impurity is still under debate. Based on many previous works, most assumed that nitrogen is the most likely candidate of donor [14–16,22–24], but there is no experimental evidence to support these proposals. Meanwhile, Su, et al. (2018) suggested iron (Fe) impurity should be the donor [25], after X-ray photoelectron spectroscopy (XPS) analysis and theoretical calculation.

Recent articles pointed out the uncompensated boron peak height increased when the type IIb diamonds were exposed to UV-light [26,27]. That is to say, when the type IIb diamond was luminesced with UV-light source, the amount of acceptor increased, so it is possible that the donors should also be released from acceptors' combination. That enlightened us that using external UV excitation on phosphorescent HPHT synthetic diamonds, we may capture some evidence of the donor in an experiment.

Guided by this assumption, a series of experiments were carried out on a batch of HPHT synthetic diamonds, using FTIR spectrometer, photoluminescence (PL) spectrometer, electron paramagnetic resonance (EPR) spectrometer and ultraviolet–visible–near infrared spectrometer. Our results suggested that neutral isolated nitrogen ( $N_0^0$ ) is forming under UV excitation. By trapping electron and recombining with acceptor (uncompensated boron), it may take part in the phosphorescence process as the donor.

## 2. Materials and method

### 2.1. Samples

Images and basic information of ten colorless HPHT synthetic diamonds are illustrated in Fig. 1 and Table 1. All the samples are

standard round brilliant cut. To collect the fine FTIR absorption spectra, a culet facet which is parallel to the table facet of diamond was cut. Thus, the optical path length equals to the thickness of the stone.

### 2.2. Instruments

#### 2.2.1. Luminescence

In a 5500 K color temperature LED light box, Nikon D810 DSLR camera was employed to photograph samples. Using a standard UV lamp with typical 365 nm for longwave UV and typical 254 nm for shortwave UV [28], samples' luminescence was checked by naked eyes firstly. Further, the luminescence images were captured by DTC DiamondView™ with UV-light shorter than 230 nm [29]. Luminescence images were captured under different parameters, including delay time, integration time, gain and aperture.

#### 2.2.2. FTIR

A Bruker v80 Hyperion 3000 micro infrared spectrometer was used to collect FTIR spectra, in order to determine the diamond types and to quantitatively describe the 2802  $\text{cm}^{-1}$  peak. The absorption spectra were obtained under the transmission measurement mode, where the spot diameter is 100  $\mu\text{m}$ , the resolution is 4  $\text{cm}^{-1}$ , the scanning range is 6000–400  $\text{cm}^{-1}$  and the number of scans is set to 64.

A JASCO FP8500 photoluminescence (PL) spectrometer equipped with a 150 W Xenon lamp ranged from 200 to 750 nm was employed to measure three-dimensional luminescence spectra in order to find the most suitable excitation wavelength. For generating three-dimensional spectra, excitation range was set as 200–250 nm with 10 nm step, while emission was collected in the range of 300–600 nm with 3 nm step. Additionally, a set of higher resolution emission spectra were collected with excitation wavelength of 230 nm and emission wavelength of 350–650 nm with 0.2 nm steps. Then, the lifetimes were fitted.

A JY HORIBA Lab RAM HR Raman spectrometer was used to measure the Raman spectra. The light source is a 30-mW He–Cd 325 nm laser. The spectrum ranges are 100–4550  $\text{cm}^{-1}$ . Depending on the results, the measurement times, integration time and power attenuation were flexible for each sample. Samples were submerged in liquid nitrogen (LN) with part of the diamonds above the LN surface till thermal equilibrium before measurement.

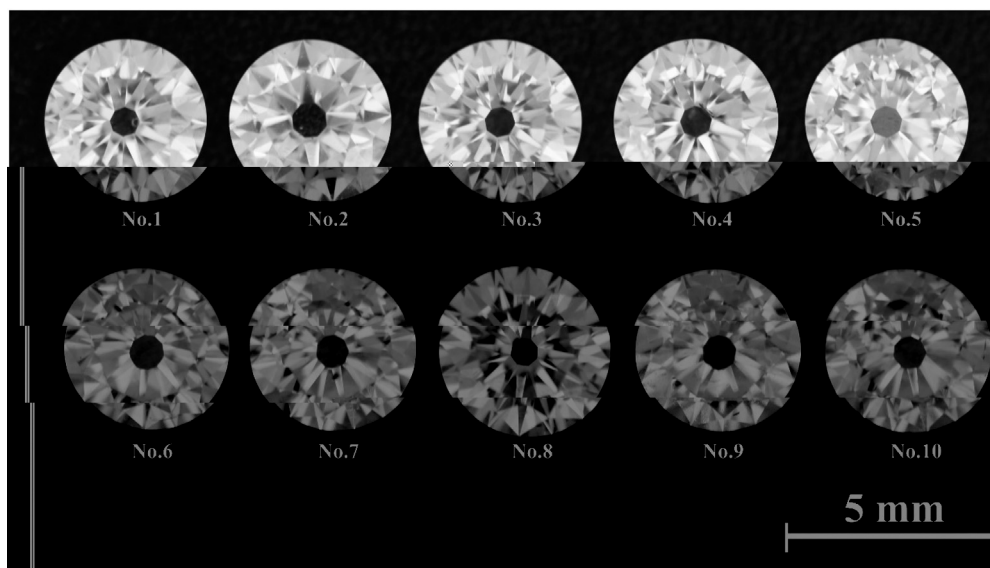


Fig. 1. Ten boron-doped high temperature high pressure synthetic diamonds.

**Table 1**  
Basic information of boron-doped HPHT synthetic diamond.

| Sample No. | Cut       | Weight /ct | Clarity | Type | Thickness /mm | Colour     | Phosphorescence Color <sup>a</sup> |       |
|------------|-----------|------------|---------|------|---------------|------------|------------------------------------|-------|
|            |           |            |         |      |               |            | LWUV                               | SWUV  |
| 1          | Round     | 0.191      | SI      | IIb  | 2.00          | Colourless | none (Inert)                       | GB    |
| 2          | Brilliant | 0.192      |         | IIb  | 1.98          |            |                                    | GB    |
| 3          |           | 0.198      |         | IIb  | 2.00          |            |                                    | GB    |
| 4          |           | 0.199      |         | IIa  | 2.00          |            |                                    | GB    |
| 5          |           | 0.206      |         | IIb  | 2.06          |            |                                    | GB    |
| 6          |           | 0.205      |         | IIb  | 2.04          |            |                                    | GB    |
| 7          |           | 0.213      |         | IIb  | 2.10          |            |                                    | GB    |
| 8          |           | 0.222      |         | IIb  | 2.10          |            |                                    | GB    |
| 9          |           | 0.205      |         | IIb  | 2.06          |            |                                    | GB    |
| 10         |           | 0.227      |         | IIb  | 2.00          |            |                                    | GB→GY |

<sup>a</sup> GB: Greenish Blue; GY: Greenish Yellow.

A JASCO MSV5200 micro ultraviolet–visible–near infrared (UV–Vis–NIR) spectrometer was operated to collect the UV–Vis–NIR spectra. Under the transmission measurement mode, the aperture was set to 100  $\mu\text{m}$ , the measurement range was set into 200–2500 nm with data interval 0.5 nm.

EPR spectra in room temperature were collected using a Bruker EMX-10/12 electron paramagnetic resonance spectrometer at X band located in Center of Material Analysis, Nanjing University. Samples were measured with and without external UV-light (Hg lamp) excitation. In order to compare both spectra, all the parameters were constant, including modulation amplitude 1 Gauss, conversion time 163.84 ms.

### 3. Results

#### 3.1. FTIR spectra

As Fig. 2 shows, except for lattice vibration near 2160, 2030 and 1974  $\text{cm}^{-1}$  [30], FTIR spectra lack 1282, 1175 and 1130  $\text{cm}^{-1}$  nitrogen-related defects [2,31,32] and 3107  $\text{cm}^{-1}$  hydrogen-related defects [33]. However, nine diamonds have absorption peak near 2931, 2802 and 2453  $\text{cm}^{-1}$ , which are all caused by uncompensated boron in diamonds [10].

Fisher et al. (2009) had established an empirical formula to determine the uncompensated boron concentration (hereinafter referred to as  $[B_0]$ ) from integral area on 2802  $\text{cm}^{-1}$  peak [11]. Following this method,  $[B_0]$  of each sample was calculated and listed in Table 2.

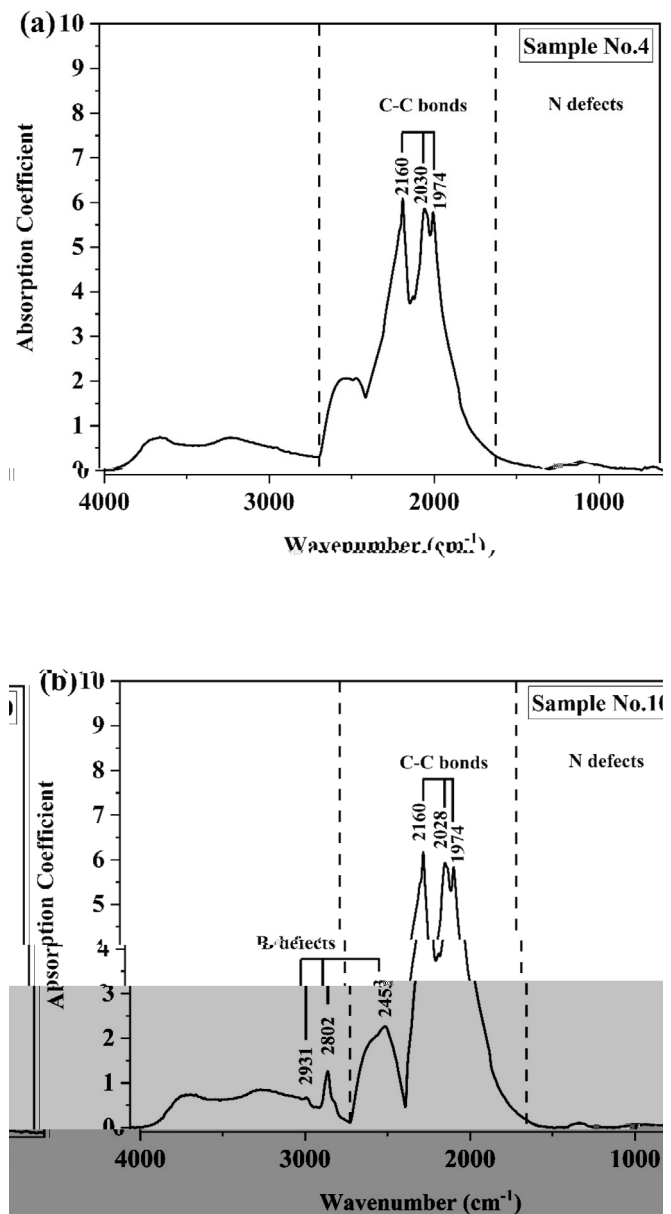
#### 3.2. Photoluminescence (PL) spectra

Fig. 3 depicted the photoluminescence images captured by DiamondView™. All the samples exhibit greenish blue luminescence. The images were taken under fluorescence mode with integral time of 1 s. We found some faint patterns or shadows inside the table facets by careful observation. These patterns are rectangles in shape, and some of them exhibit four arms stretching along the diagonal. These features are typical for HPHT synthetic diamonds [12].

#### 3.3. Luminescence spectra

A typical three-dimensional luminescence spectrum of these samples is given in Fig. 4 (a). Shortwave UV-light ranged from 215 to 240 nm excites the luminescence band centered at 470 nm, which extends from 370 to 600 nm.

As in Fig. 4 (b), an emission spectrum ( $\lambda_{\text{exc}} = 230 \text{ nm}$ ) shows a band centered at 470 nm and a shoulder near 500 nm. The 500 nm shoulder implies the existence of 500 nm band mentioned in other



**Fig. 2.** FTIR spectra of diamonds without any detectable nitrogen- and hydrogen-related defects. (a) Sample No.4 is a type IIa diamond without boron related band; (b) Sample No.10 is a type IIb diamond that contains strongest 2802  $\text{cm}^{-1}$  band among all samples.

**Table 2**  
Concentrations of uncompensated boron in our samples.

| Sample No.                 | 1     | 2     | 3     | 4                | 5     | 6     | 7     | 8     | 9     | 10    |
|----------------------------|-------|-------|-------|------------------|-------|-------|-------|-------|-------|-------|
| Peak area/cm <sup>-2</sup> | 15.99 | 14.06 | 10.21 | bdl <sup>a</sup> | 2.66  | 19.53 | 8.078 | 33.44 | 33.35 | 46.28 |
| B uncompensated/ppm        | 0.009 | 0.008 | 0.006 | bdl              | 0.002 | 0.011 | 0.005 | 0.019 | 0.018 | 0.026 |

<sup>a</sup> bdl: below the detection limit

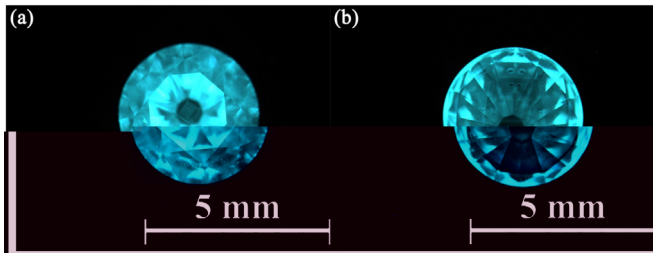


**Fig. 3.** (a) Luminescence image of sample No.5 which contains an obvious rectangle shadow in the middle of the table; (b) Luminescence image of sample No.3 presents two stretching arms.

works [16,23]. The shape of the band is asymmetrical. Additionally, we also determined the lifetime of this emission band. Generally, lifetime ( $\tau$ ) is the timespan when phosphorescence intensity decays from 100% to 37% [34]. By fitting exponential function ( $I = A e^{-t/\tau} + B_0$ ), the phosphorescence lifetime of 470 nm emission band was determined. Results are shown in Table 3 and Fig. 5. Data suggest that the lifetime of 470 nm phosphorescence is negatively correlated to  $[B_0]$ .

### 3.4. Raman spectra

Typical 325 nm laser Raman spectra were shown as Fig. 6. Both samples have the Raman intrinsic peak near 1332 cm<sup>-1</sup> [30].

### 3.5. UV-Vis absorption spectra

In Fig. 7, both samples have the similar absorption edge near 5.5 eV, which indicated that they are type II diamonds. That also support what we observed in Fig. 4(a), that the photoluminescence can be emitted only when the excitation light's wavelength is close to ~230 nm.

### 3.6. EPR spectra

Fig. 8 (a) shows the EPR spectra of sample No.4, before (red) and during (black) the external UV-light excitation. Fig. 8 (b) shows the similar ERP spectra of sample No.10, during (black) and after (red) the external UV-light excitation. The different split is caused by different direction with magnetic field.

Without UV-light irradiation, neither of samples exhibited any detectable signal. However, when diamond was exposed to Hg lamp for about 60 s, signals arose. When phosphorescence stops completely, the signal disappeared. All the detectable signal shared the same g-value. These results clearly pointed out that the UV-light excitation produced paramagnetic electron.

## 4. Discussion

### 4.1. Identification of the 470 nm band

In previous works [4,16,22,23], the 500 nm phosphorescence band was reported and confirmed, but band centered in 470 nm

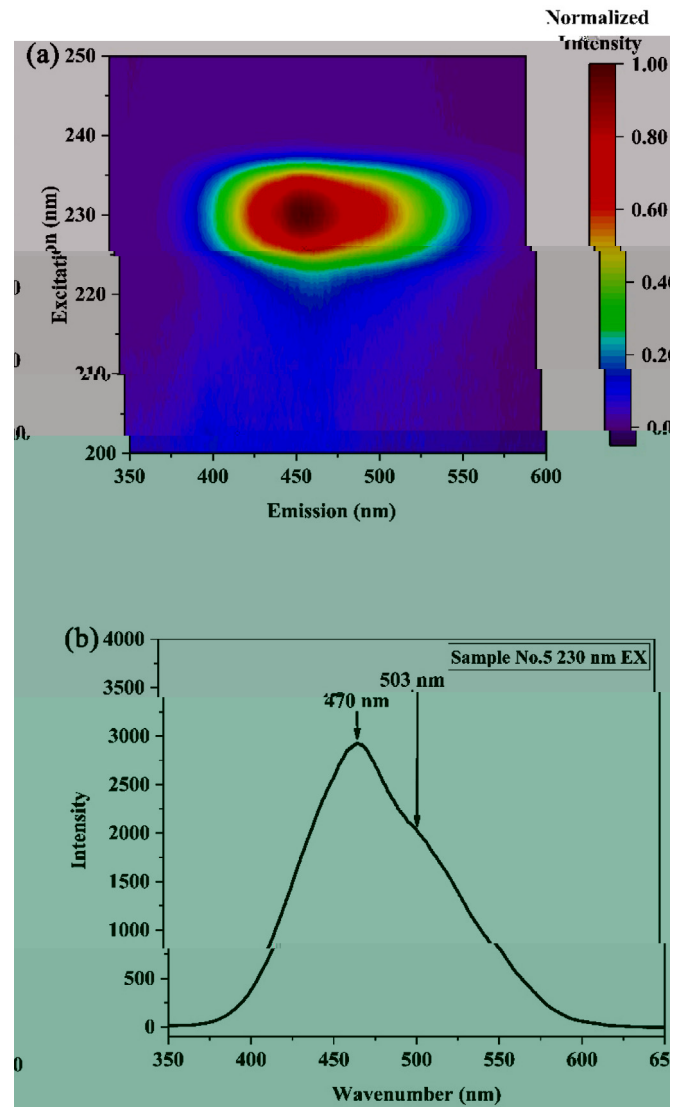


**Fig. 4.** Photoluminescence spectra with a xenon lamp excitation. (a) Three-dimensional photoluminescence spectrum of sample No.10. The spectrum has a band centered in 470 nm best excited by 230 nm ultraviolet light. (b) Photoluminescence emission spectrum of sample No.5. The spectrum has a band centered in 470 nm with a shoulder near 500 nm.

was also mentioned in some articles [24,25]. According to the following reasons, we suggested 470 nm band in our samples is also a DAP band and it comes from the same mechanism as the 500 nm band.

Firstly, the typical shape and peak position in our spectra (Fig. 4) is accordance with the spectrum from prior study [25] and they both obey the DAPR equation. Secondly, our measurements and observation revealed that the  $[B_0]$  correlated lifetime of 470 nm band negatively. This correlation is similar to what Watanabe et al.

**Table 3**  
[B<sub>0</sub>] and 470 nm band lifetime of all samples (order by [B<sub>0</sub>]).

| Sample No.            | 4    | 5     | 7     | 3     | 2     | 1     | 6     | 9     | 8     | 10    |
|-----------------------|------|-------|-------|-------|-------|-------|-------|-------|-------|-------|
| [B <sub>0</sub> ]/ppm | bdl  | 0.002 | 0.005 | 0.006 | 0.008 | 0.009 | 0.010 | 0.018 | 0.019 | 0.026 |
| Lifetime/s            | 18.1 | 14.1  | 16.3  | 18.9  | 14.7  | 9.3   | 11.5  | 8.9   | 5.2   | 8.9   |
| S.E. <sup>a</sup>     | 0.83 | 0.55  | 0.84  | 1.02  | 0.56  | 0.27  | 0.32  | 0.28  | 0.12  | 0.20  |

<sup>a</sup> S.E.: Standard Error

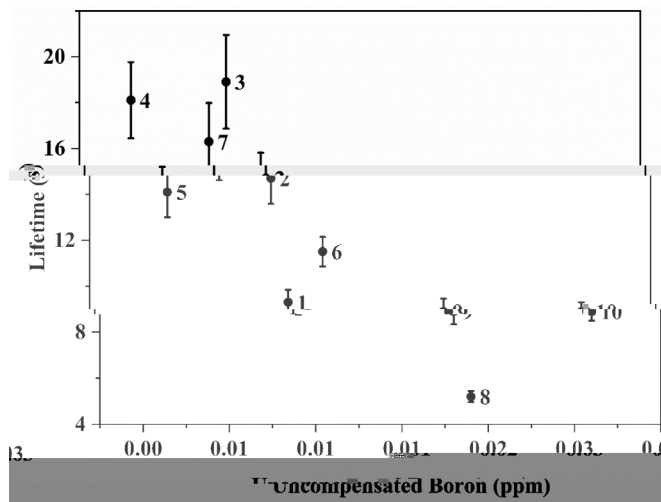


**Fig. 5.** The relationship between 470 nm phosphorescence lifetimes and [B<sub>0</sub>]. Sample No.4 without uncompensated boron has an 18-s lifetime; Sample No.8 with 0.019 ppm [B<sub>0</sub>] has a 5-s lifetime.

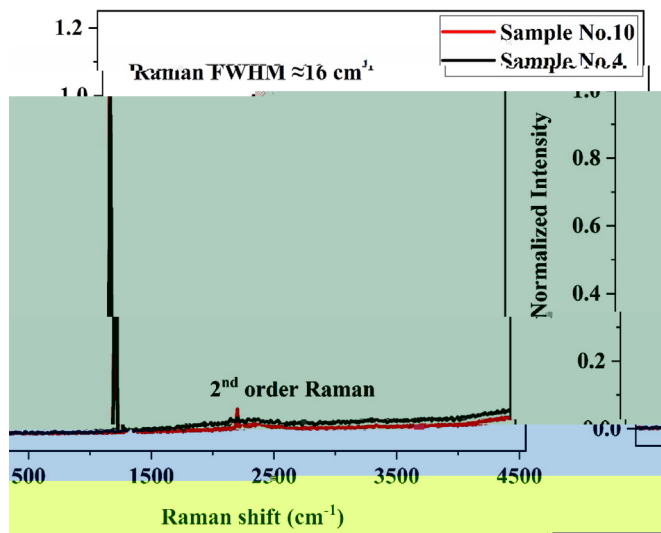


**Fig. 6.** Raman spectrum of sample No.4 and No.10. (A colour version of this figure can be viewed online.)

(1997) [16] and Eaton-Magaña et al. (2011) [23] found on 500 nm band. Last but not the least, we observed a shoulder near 500 nm along with 470 nm band in our spectrum (Fig. 4). There is an important parameter *r* in Eq. 1, which is inversely proportional to *E<sub>0</sub>r<sup>3</sup>* and donor-acceptor pairs may occur at different distances [24], when pairs with a specific distance *r* are dominant in a sample, the phosphorescence band would be centered in corresponding *E<sub>0</sub>r<sup>3</sup>*. Thus, the presence of 470 nm and 500 nm shoulder can be explained as the result of donor-acceptor-pair with different

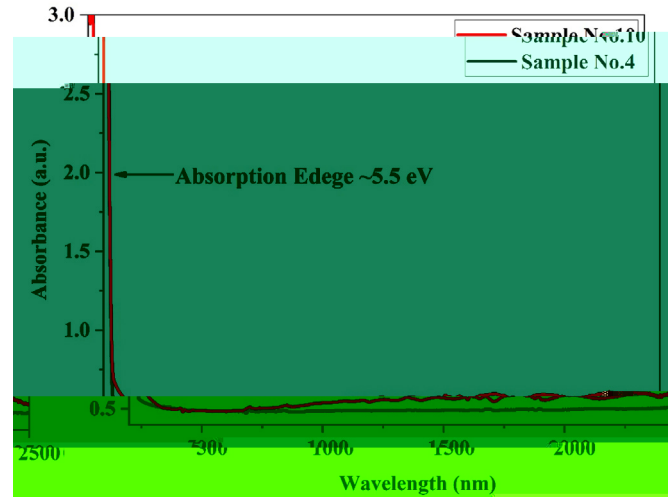


**Fig. 7.** UV-Vis-NIR spectra of No.4 and 10. (A colour version of this figure can be viewed online.)

distance distribution.

#### 4.2. A *d* 470 *d*

Former models [14–16] pointed out that phosphorescence from type IIb diamonds could be explained by DAPR theory, which had been mentioned in the introduction part. The detailed excitation process is described as following:

Before the excitation, donor and acceptor with proper distances can be charge-compensated and become ionized, resulting in a donor-acceptor pair. When excited by UV-light, electrons in valence band get excited and captured by “ionized donors”, leaving holes behind in the valence band. These remaining holes in the valence band will be totally captured by “ionized acceptors” sooner or later. The result of such process will be that ionized donors and acceptors eventually become neutral (when the external excitation source remains). Then neutral donors and acceptors got recombined, releasing photons of the phosphorescence [16,19]. Considering the negative correlation between impurities distance and impurities concentration, a modified equation is given [16]:

$$E_{0r^3} \propto \left( \frac{1}{d} - \frac{1}{d_0} \right) \propto \frac{202\pi}{\epsilon} \frac{p^{\frac{1}{3}}}{\epsilon}, \quad \text{Eq.2}$$

where *E<sub>0</sub>r<sup>3</sup>* is the phosphorescent photon energy, *E<sub>g</sub>*, *E<sub>a</sub>* and *E<sub>d</sub>* are bandgap of diamond, binding energy of acceptor and binding energy of donor respectively, *e* is the electron charge, *p* is the higher value of the acceptor or donor concentration, and *ε* is the static dielectric constant of diamond. For *E<sub>g</sub>* 5.47 eV, *E<sub>a</sub>* 0.37 eV, and the phosphorescent energy of 470 nm band *E<sub>0</sub>r<sup>3</sup>* 2.64 eV, we can figure out that *d<sub>0</sub>* ≈ 2.54 nm.

To make this model reasonable, we need to find out which impurity, with a binding energy of 2.54 eV, acts as the donor during the phosphorescence process.

4.2.1. . d . . . . . d .

valence band got excited, leaving holes behind. Ionized isolated nitrogen captured these excited electrons, while ionized boron captured the holes in valence band subsequently, resulting in neutral isolated nitrogen and neutral boron. Then the neutral isolated nitrogen and neutral boron recombined, generating phosphorescence. If there were any extra uncompensated boron, they would create extra holes in valence band, and then these holes would be captured by ionized boron. That means the total number of holes exceeds the total number of electrons during the phosphorescence process. So, the recombination process would be accelerated and phosphorescence lifetime would be decreased. The mechanism on 470 nm phosphorescence is illustrated in Fig. 9.

#### 4.3. Discussion

Although the experimental method applied in this study performed well on detecting  $N_5^0$  and providing a good support to DAPR model explaining the phosphorescence in HPHT synthetic type IIb diamonds, some questions are still open.

Math add-up problem remains a significant one. The inferred activation energy of donor is numerically different from the experimental value. Most researchers (including us) introduced a relaxation energy to adjust the outcomes. So, a detailed theoretical calculation on nitrogen-boron pair is required in the future.

There are other factors without being considered in this model, such as temperature, different growth sectors and so on, which may influence the lifetime and other properties on phosphorescence. Although it is beyond the consideration of this study, but still makes an problem in application of DAPR model in diamond.

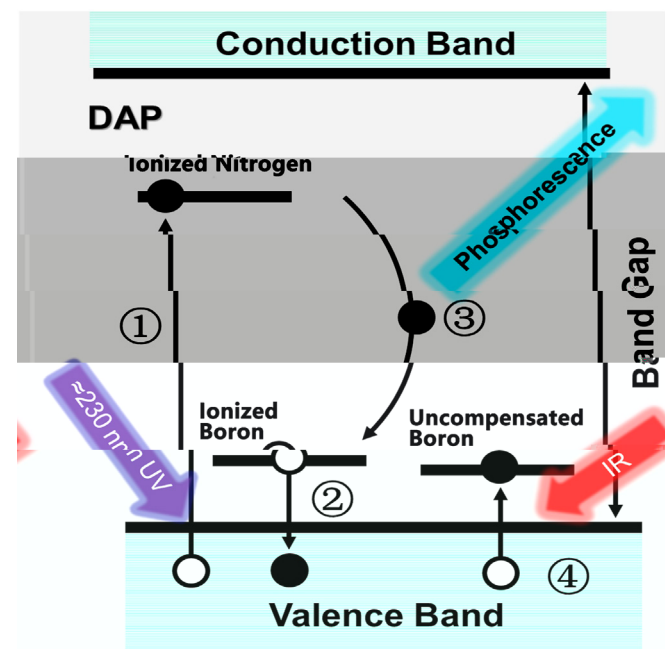


**Fig. 9.** The concise mechanism model of 470 nm band in our samples (modified after reference [16]). The solid dot represents electron and hollow dot represents hole. On one hand, nitrogen and boron were charge compensated with each other and got ionized. On the other hand, uncompensated boron can capture electron from valence band by absorbing infrared. ①When UV-light irradiated diamond,  $N_5^0$  can trap an electron from valence band to become  $N_5^+$  which has EPR signal. ②Then the hole left in valence band would become filled with an electron from  $B^0$  to make  $B^+$ . ③Thirdly,  $N_5^+$  and  $B^+$  would recombine with phosphorescence emission. ④Meanwhile, uncompensated boron can provide extra holes in valence band which would accelerate the recombination process between  $N_5^+$  and  $B^+$ . (A colour version of this figure can be viewed online.)

## 5. Conclusions

All the boron-doped HPHT synthetic diamonds used in this work can emit greenish blue phosphorescence centered around 470 nm after being exposed to shortwave UV-light of 215–240 nm. Such phosphorescence can be explained by DAPR theory, where the acceptor is widely believed to be boron.

By EPR experiments, we propose that isolated nitrogen is probably the donor in DAPR model of type IIb diamond. Thus, the model, where the isolated nitrogen takes the role of donor and boron acts as acceptor is suggested: generally, isolated nitrogen and boron combine to be a pair; when these diamonds are irradiated by UV-light, electrons and holes become trapped by isolated nitrogen and boron respectively, then the pair “separates”; when the recombination of separated isolated nitrogen and boron takes place, phosphorescence releases.

### CRedit authorship contribution statement

**Tian Shao:** Conceptualization, Methodology, Writing - original draft, Investigation, Data curation. **Fanglin Lyu:** Conceptualization, Writing - original draft, Investigation, Data curation. **Xuwen Guo:** Investigation, Resources. **Jinju Zhang:** Investigation. **Haikun Zhang:** Investigation. **Xin Hu:** Resources, Supervision. **Andy H. Shen:** Supervision, Project administration, Writing - review & editing.

### Declaration of competing interest

The authors declare that they have no known competing financial interests or personal relationships that could have appeared to influence the work reported in this paper.

### Acknowledgement

We acknowledge the National Key R&D Program of China (#2018YFF0215403) for the financial support to this research. This paper is GIC contribution CIGTWZ-2020010. We also thank Dr. Sally C Eaton-Magaña of Gemology Institute of America (GIA), doctoral candidate Ms. Jiahui Zhao of Warwick University and Dr. Gai Wu of Wuhan University for their valuable discussions.

### References

- [1] T. Hainschwang, E. Fritsch, F. Notari, B. Rondeau, A. Katruscha, The origin of color in natural c center bearing diamonds, *Diam. Relat. Mater.* 39 (2013) 27–40.
- [2] C.M. Breeding, J.E. Shigley, The “Type” classification system of diamonds and its importance in gemology, *Gems Gemol.* 45 (2) (2009) 96–111.
- [3] E. Gaillou, G.R. Rossman, Color in natural diamonds: the beauty of defects, *Rocks Miner.* 89 (1) (2014) 66–75.
- [4] J.E. Post, F. Farges, The hope diamond: rare gem, historic jewel, *Rocks Miner.* 89 (1) (2014) 16–26.
- [5] E. Gaillou, J.E. Post, K.S. Byrne, J.E. Butler, Study of the blue moon diamond, *Gems Gemol.* 50 (4) (2014) 280–286.
- [6] J.F.H. Custers, Unusual phosphorescence of a diamond, *Physica* 18 (8–9) (1952) 489–496.
- [7] J.F.H. Custers, Semiconductivity of a type IIb diamond, *Nature* 176 (4473) (1955) 173–174.
- [8] I.G. Austin, R. Wolfe, Electrical and optical properties of a semiconducting diamond, *Proc. Phys. Soc. B* 69 (3) (1956) 329–338.
- [9] T.P. Wedepohl, Electrical and optical properties of type IIb diamonds, *Proc. Phys. Soc. B* 70 (2) (1957) 177–185.
- [10] A.T. Collins, A.W.S. Williams, The nature of the acceptor centre in semiconducting diamond, *J. Phys. C Solid State Phys.* 4 (1971) 1789–1800.
- [11] D. Fisher, S.J. Sibley, C.J. Kelly, Brown colour in natural diamond and interaction between the brown related and other colour-inducing defects, *J. Phys. Condens. Matter: an Institute of Physics journal* 21 (36) (2009) 364213.
- [12] J.E. Shigley, E. Fritsch, I. Reinitz, T. Moses, A chart for the separation on natural and synthetic diamonds, *Gems Gemol.* 31 (4) (1995) 256–264.
- [13] J. Isoya, H. Kanda, Y. Uchida, EPR studies of interstitial Ni centers in synthetic

- diamond crystals, *Phys. Rev. B* 42 (16) (1990) 9843–9852.
- [14] P.J. Dean, Bound excitons and donor-acceptor pairs in natural and synthetic diamond, *Phys. Rev.* 139 (2A) (1965) A588–A602, 139(2A).
- [15] P.B. Klein, M.D. Crossfield, J.A. Freitas Jr., A.T. Collins, Donor-acceptor pair recombination in synthetic type-IIb semiconducting diamond, *Phys. Rev. B* 51 (15) (1995) 9634–9642.
- [16] K. Watanabe, S.C. Lawson, J. Isoya, H. Kanda, Y. Sato, Phosphorescence in high-pressure synthetic diamond, *Diam. Relat. Mater.* 6 (1) (1997) 99–106.
- [17] S.C. Eaton-Magaña, J.E. Post, P.J. Heaney, J. Freitas, P. Klein, R. Walters, et al., Using phosphorescence as a fingerprint for the Hope and other blue diamonds, *Geology* 36 (1) (2008) 83–86.
- [18] D.G. Thomas, M. Gershenson, F.A. Trumbore, Pair spectra and "edge" emission in gallium phosphide, *Phys. Rev.* 133 (1A) (1964) A269–A279.
- [19] D.G. Thomas, J.J. Hopfield, W.M. Augustyniak, Kinetics of radiative recombination at randomly distributed donors and acceptors, *Phys. Rev.* 140 (1A) (1965) A202–A220.
- [20] E.F. Apple, F.E. Williams, Associated donor-acceptor luminescent centers in zinc sulfide phosphors, *The Electrochemical Society* 106 (3) (1959) 224–230.
- [21] R.M. Chrenko, Boron, the dominant acceptor in semiconducting diamond, *Phys. Rev. B* 7 (10) (1973) 4560–4567.
- [22] J.A. Freitas, P.B. Klein, A.T. Collins, Evidence of donor-acceptor pair recombination from a new emission band in semiconducting diamond, *Appl. Phys. Lett.* 64 (16) (1994) 2136–2138.
- [23] S.C. Eaton-Magaña, R. Lu, Phosphorescence in type IIb diamonds, *Diam. Relat. Mater.* 20 (7) (2011) 983–989.
- [24] B. Dischler, W. Rothemund, C. Wild, R. Locher, H. Biebl, P. Koidl, Resolved donor-acceptor pair-recombination lines in diamond luminescence, *Phys. Rev. B* 49 (3) (1994) 1685–1689.
- [25] L.X. Su, C.X. Zhao, Q. Lou, C.Y. Niu, C. Fang, Z. Li, et al., Efficient phosphorescence from synthetic diamonds, *Carbon* 130 (2018) 384–389, 2018.
- [26] S.C. Eaton-Magaña, Decay kinetics of boron-related peak in IR absorption of natural diamond, *Gems Gemol.* 52 (4) (2016) 412–413.
- [27] J.J. Li, C.X. Fan, Y.F. Cheng, S.X. Chen, G.H. Li, M.M. Tian, Direct evidence of charge transfer at boron acceptors being linked to phosphorescence in diamond, *Spectrosc. Spectr. Anal.* 37 (6) (2017) 1714–1717.
- [28] Y. Luo, C.M. Breeding, Fluorescence produced by optical defects in diamond: measurement, characterization, and challenges, *Gems Gemol.* 49 (2) (2013) 82–97.
- [29] C.M. Welbourn, M. Cooper, P.M. Spear, De beers natural versus synthetic diamond verification instruments, *Gems Gemol.* 32 (3) (1996) 156–169.
- [30] B. Dischler, *Handbook of Spectral Lines in Diamond*, ume 1, Springer-Verlag Berlin and Heidelberg GmbH & Co., New York, 2012. Tables and Interpretations.
- [31] G.S. Woods, G.C. Purser, A.S.S. Mtimkkulu, A.T. Collins, The nitrogen content of natural type Ia diamonds, *J. Phys. Chem. Solid.* 51 (10) (1990), 1911–1197.
- [32] W.R. Taylor, A.L. Jaques, M. Ridd, Nitrogen-defect aggregation characteristics of some australasian diamonds: time-temperature constraints on the source regions of pipe and alluvial diamonds, *Am. Mineral.* 75 (11) (1990) 1290–1310.
- [33] F. De Weerd, A.T. Collins, Optical study of the annealing behaviour of the 3107  $\text{cm}^{-1}$  defect in natural diamonds, *Diam. Relat. Mater.* 15 (4–8) (2006) 593–596.
- [34] J.R. Lakowicz, *Principles of Fluorescence Spectroscopy*, third ed., Springer, New York, 2006.
- [35] W.V. Smith, P.P. Sorokin, I.L. Gelles, G.J. Lasher, Electron-spin resonance of nitrogen donors in diamond, *Phys. Rev.* 115 (6) (1959) 1546–1552.
- [36] S.C. Lawson, D. Fisher, D.C. Hunt, M.E. Newton, On the existence of positively charged single-substitutional nitrogen in diamond, *J. Phys. Condens. Matter* 10 (27) (1998) 6171–6180.
- [37] R. Jones, J.P. Goss, P.R. Briddon, Acceptor level of nitrogen in diamond and the 270-nm absorption band, *Phys. Rev.* 80 (3) (2009), 033205.033201-033205.033204.
- [38] R. Ulbricht, S.T. Van d Post, J.P. Goss, R. Jones, R.U.A. Khan, M. Bonn, Single substitutional nitrogen defects revealed as electron acceptor states in diamond using ultrafast spectroscopy, *Phys. Rev. B* 84 (16) (2011) 165202. *Physical Review B*. 84 (16) (2011) 165202.165201-165202.165209.
- [39] A.M. Ferrari, S. Salustro, F.S. Gentile, W.C. Mackrodt, R. Dovesi, Substitutional nitrogen atom in diamond. A quantum mechanical investigation of the electronic and spectroscopic properties, *Carbon* 134 (2018) 354–365, 2018.
- [40] K. Iakoubovskii, G.J. Adriaenssens, Optical transitions at the substitutional nitrogen centre in diamond, *J. Phys. Condens. Matter* 12 (6) (2000) L77–L81.
- [41] U.F. D'Haenens-Johansson, K.S. Moe, P. Johnson, S.Y. Wong, R. Lu, W.Y. Wang, Near-colorless HPHT synthetic diamonds from AOTC Group, *Gems Gemol.* 50 (1) (2004) 30–45.
- [42] R.G. Farrer, On the substitutional nitrogen donor in diamond, *Solid State Commun.* 7 (9) (1969) 685–688.
- [43] M.H. Nazare, P.W. Mason, G.D. Watkins, H. Kanda, Optical detection of magnetic resonance of nitrogen and nickel in high-pressure synthetic diamond, *Phys. Rev. B* 51 (23) (1995) 16741–16745.